



HDAC1 suppresses radiotherapy sensitivity in cervical cancer via regulating HIF-1 α /VEGF signaling pathway

Li Liu^{1,2}, Ke Gu^{1*}, Dong Hua^{3*}

¹Department of Radiation Oncology, The Affiliated Hospital of Jiangnan University, Wuxi 214000, Jiangsu, China

²Wuxi School of Medicine, Jiangnan University, Wuxi 214000, Jiangsu, China

³Department of Oncology, The Affiliated Wuxi People's Hospital of Nanjing Medical University, Wuxi 214023, Jiangsu, China

ARTICLE INFO

Original paper

Article history:

Received: June 03, 2023

Accepted: September 01, 2023

Published: November 15, 2023

Keywords:

Cervical cancer; Radiotherapy sensitivity; HDAC1; HIF-1 α /VEGF signaling pathway

ABSTRACT

Cervical cancer (CC) is the fourth most common cancer among females worldwide. Histone deacetylase (HDAC) 1 plays a vital role in several tumors. Nevertheless, its potential and mechanism in radiotherapy sensitivity underlying CC remains obscure. Hence, the objective of this research was to probe the potential of HDAC1 in CC radiotherapy sensitivity and its mechanism of action. The expression HDACs and survival analysis of HDAC1 were investigated based on the GEPIA database. Immunohistochemical staining was implemented to detect HDAC1 and Ki-67 expression in tumor tissues. RT-qPCR and Western blot were conducted to assess HDAC1, HIF-1 α , VEGFA, along with VEGFR expressions in CC cells and tumor tissues. Cell viability, apoptosis, invasion, migration, along with cell cycle were analyzed by functional assays. Tumor-bearing nude mice model was established, and the tumor weight and volume were determined. HDAC1 was high-expressed in the tumor tissue and CC cells. In vitro, overexpression of HDAC1 suppressed radiotherapy sensitivity in C33A cells, while knockdown of HDAC1 promoted radiotherapy sensitivity in SiHa cells. In vivo, we found that HDAC1 silence hindered tumor growth and cell proliferation and promoted tumor cell apoptosis in nude mice after radiotherapy. In addition, we found that HDAC1 impacted radiotherapy sensitivity by modulating the HIF-1 α /VEGF signaling pathway. In conclusion, HDAC1 suppressed the radiotherapy sensitivity of CC via regulating HIF-1 α /VEGF signaling pathway, suggesting that HDAC1 may act as a crucial participant in regulating CC radiosensitivity, which may provide a novel method for treating CC.

Doi: <http://dx.doi.org/10.14715/cmb/2023.69.11.20>

Copyright: © 2023 by the C.M.B. Association. All rights reserved.



Introduction

The occurrence of cervical cancer (CC) has the fourth highest incidence of female malignancies worldwide, which poses a serious threat to women's health (1). The early clinical manifestations of CC are vaginal bleeding and vaginal discharge. In the late stage, there may be different secondary symptoms such as frequent urination, urgency, constipation, lower limb swelling and pain (2). The risk factors of CC include HPV infection, sexual behavior and number of deliveries, chlamydia trachomatis, herpes simplex virus type II, trichomonas infection and smoking (3). The pathological types of CC are mainly squamous cell carcinoma, adenocarcinoma and adenosquamous carcinoma (4). The treatment of CC mainly includes surgery, radiotherapy and chemotherapy (5). Clinically, radiotherapy is the most common treatment for CC, the foremost choice for locally advanced CC, and the major postoperative adjuvant treatment for early CC (6). Due to tumor heterogeneity, some tumor cells have innate radioresistance or multiple fractional irradiations induce acquired radioresistance, resulting in radiotherapy failure in some CC patients. Local uncontrolled and distant metastasis resulting from radiotherapy resistance is a major reason for the poor prognosis of CC patients (7). Hence, unveiling the

molecular mechanisms underlying CC radiotherapy resistance is necessary, in order to improve the radiosensitivity of CC patients.

Histone deacetylases (HDACs) belong to a kind of proteases that exert critical functions in chromosome structural modification and gene expression regulation. They take part in multiple physiological together with pathological processes of cells, such as regulating DNA transcription, protein synthesis, DNA damage and repair (8). Numerous literatures have displayed that HDACs are implicated in various processes of tumor development including CC (9). HDAC10 inhibits CC metastasis by inhibiting MMP-2 and -9 expression (10). L- and D-lactate modulates anticancer drug resistance in CC by inhibiting HDAC and HCAR1 activation (11). Cinnamic acid derivatives promote colon and CCs cell death by inhibiting HDACs expression (12). These findings suggested that targeting HDACs may offer a novel approach to radiotherapy in CC.

Hypoxia is one of the key features of most solid cancers, CC included (13). Hypoxia can stabilize hypoxia-inducible factor-1 α (HIF-1 α) (14). HIF-1 α stimulates the expression of its target genes such as vascular endothelial growth factor (VEGF), which can induce angiogenesis (15). It is well known that the HIF-1 α /VEGF signaling axis is involved in CC (16). On the basis of The Cancer

* Corresponding author. Email: drduke@jiangnan.edu.cn; wx89211@163.com

Genome Atlas (TCGA) database, HDAC1 expression is discovered to be increased in most tumors, CC included. Besides, previous literatures have suggested that HDAC1 is involved in modulating the progression of breast cancer (17), colorectal cancer (18) and pediatric liver cancer (19). Survival curve analysis exhibits that the low expression of HDAC1 harbors a good survival rate, mirroring that HDAC1 plays a vital role in promoting CC progression. Furthermore, abnormal expression of HDAC1 in CC is observed. Ali et al. have shown that sulforaphane is involved in modulating several tumor suppressor genes expression by targeting DNMT3B and HDAC1 in CC cells (20). Sixto-López et al. have indicated that HO-AAVPA increases the translocation of HMGB1 levels and inhibits HDAC1 expression in CC cells (21). Nevertheless, the detailed function and mechanism of HDAC1 underlying the radiotherapy resistance of CC are still obscure. Therefore, this research was intended to explore the mechanism of HDAC1 in radiotherapy sensitivity underlying CC to provide a new molecular target for radiotherapy in CC.

Materials and Methods

Tumor tissues collection and ethics statement

A total of 10 CC tissues and the corresponding adjacent noncancerous tissue (NCT) were acquired from patients who underwent surgery from 2018 to 2022 at The Affiliated Hospital of Jiangnan University. Tissue samples were preserved at -80 °C. The present research was approved by the Medical Ethics Committee of Jiangnan University and complied with the Declaration of Helsinki. All patients signed informed consent.

Cell culture, transfection, and treatment

Human normal cervical endothelial cells, H8 and CC cell lines (HeLa, Siha, Caski and C33A), were obtained from Crondabio. H8 cells were cultivated in minimum Eagle's medium (MEM, BL306A, Biosharp). HeLa and Siha cells were cultivated in Dulbecco's modification of Eagle's medium (DMEM, BL301A, biosharp). Caski and C33A cells were cultivated in RPMI-1640 medium (DMEM, BL303A, biosharp). All the above mediums were added with 10% fetal bovine serum (FBS) at 37 °C with 5% CO₂. For transfection, the overexpressing HDAC1 plasmid and siRNA of HDAC1 (Invitrogen, USA) were transfected into CC cells using Lipofectamine 2000 Transfection Reagent (Thermo Fisher Scientific, Waltham, USA). For radiological treatment, the cells or transfected cells were treated by 60-cobalt gamma-ray irradiation with 0, 2, 4, 6, and 8 Gy doses. The sequences of siRNA of HDAC1 as follows: Si-HDAC1-1, Sense: 5'-GCUUCAAUCUAACUAUCAAAG-3', antisense: 5'-UU-GAUAGUUAGAUUGAAGCAA-3'; Si-HDAC1-2, Sense: 5'-CAGCGAUGACUACAUAUAAAUU-3', antisense: 5'-UUUAAUGUAGUCAUCGCUGUG-3'; Si-HDAC1-3, Sense: 5'-CGACUGUUUGAGAACC UUAGA-3', antisense: 5'-UAAGGUUCUCAACA-GUCGCU-3'.

RNA extraction and qRT-PCR

Isolation of total RNA from cells and cervical tissues was implemented using TRIzol (BS259A, Biosharp). A total of 1 μ g RNA was reverse-transcribed into cDNA using a Hifair® II Enzyme Mix Kit (KCD-M1003, Crondabio).

The RT-PCRs were implemented using the SYBR Green qPCR Master Mix (KCD-M1004, Crondabio) by the Light-Cycler® 480II real-time PCR system (Roche). The β -actin was used as an internal control. The calculation of gene expression was implemented using the 2^{- $\Delta\Delta$ Ct} method. The primers used in the present study were as follows: actin, Forward: 5'-ACGTGGACATCCGCAAAG-3'; Reverse: 5'-TGGAAGGTGGACAGCGAGGC-3'; HDAC1, Forward: 5'-CGCCCTCACAAAGCCAATG-3'; Reverse: 5'-CTGCTTGCTGTACTCCGACA-3'; HIF-1 α , Forward: 5'-GAACGTCGAAAA-GAAAAGTCTCG-3'; Reverse: 5'-CCTTATCAAGATGCGAACTCACA-3'; VEGFA, Forward: 5'-AGGGCAGAATCATCAC-GAAGT-3'; Reverse: 5'-AGGGTCTCGATTGGATG-GCA-3'; VEGFR, Forward: 5'-GTGATCGGAAATGACTGTG-GAG-3'; Reverse: 5'-CATGTTGGTCACTAACA-GAAGCA-3'.

Western blot analysis

Total protein was extracted from the cells and tumor tissues by radioimmunoprecipitation assay buffer (BL504A, Biosharp), followed by the determination of total protein concentration using the BCA Protein Assay Kit (BL521A, Biosharp). A total of 30 μ g protein was used for SDS-PAGE and then transferred onto polyvinylidene difluoride membranes (PVDFM, IPVH00010, Millipore). The membranes were incubated with primary antibody anti-HDAC1 (1:4000 dilution; 66085-1-Ig, Proteintech), anti-HIF-1 α (1:4000 dilution, BF8002, Affinity), anti-VEGFA (1:4000 dilution; 19003-1-AP, Proteintech), anti-VEGFR (1:4000 dilution; 26415-1-AP, Proteintech) and anti-actin (GB11001; Servicebio) overnight at 4 °C after blocked by 5% dried skimmed milk at room temperature for 1 h. Furthermore, the membrane was incubated with a secondary antibody, goat anti-rabbit IgG antibody, conjugated with horseradish peroxidase (HRP) (1:5000 dilution, ab205718, Abcam) at room temperature for 1 h. The protein signals were visualized with the Enhanced Chemiluminescence Kit (ECL, WBKLS0100, Millipore) using ChemiDocXRS+ (Bio-Rad).

Cell counting kit-8 (CCK-8) assay

In total, 3 \times 10⁴ cells/mL Siha and C33A cells were seeded separately in 96-well plates and treated with overexpressing HDAC1 plasmids and siRNA of HDAC1 for 36 h. Subsequently, radiological treatment was performed at 8 Gy for 12 h. Moreover, 15 μ L of the CCK-8 stain (PR645, Dojindo) was added to each well. The cells were incubated for another 2 h. After that, the optical density was detected using a microplate reader (VARIOSKAN LUX, Thermo Scientific) at 450 nm wavelength.

Transwell assay

Next, 25 μ L Matrigel (354234, BD) was covered to the upper chamber of the Transwell plate (3422, Corning), the whole polycarbonate film was covered, and the Matrigel was polymerized into glue at 37 °C for 30 min. Furthermore, CC cells were inoculated into the upper chamber. For Siha and C33A cells, 8 Gy radiation was performed after transfection for 36 h. After 24 h incubation, non-invading cells were gently removed with a cotton swab. The invaded cells were fixed with 4% polymethyl alcohol

for 30 min, washed twice with phosphate-buffered saline (PBS), and dyed with crystal violet for 10 min. The number of invading cells was determined under a light microscope DMI8 (Leica).

Scratch test

Siha and C33A cells in the logarithmic growth period were planted into 6 cm dishes, and the cell density was set to 80%. Before cell radiation, cell scratches were made using 200 μ L pipette tips, and the width of each scratch was kept consistent as far as possible. The cell culture solution was sucked out, the pore plate was washed with PBS thrice, and the cell fragments generated by scratches were removed. The migrating cells were determined under a light microscope DMI8 (Leica) with the same scribing position of each group of cells at 0 and 12 h. The migration distance of each group of cells was analyzed quantitatively with ImageJ software.

Tube formation experiment

Siha and C33A cells were obtained in the logarithmic growth phase. Afterward, 10 μ L refrigerated tip and μ -slide angiogenesis were removed from the freezer, and 10 μ L of Matrigel was treated into each well of the μ -slide. After adding the Matrigel, the μ -slide was put into a petri dish of suitable size. Then, the entire petri dish was placed in the incubator to solidify. During gelling, the cells were digested and collected after 12 h, and the cell concentration was adjusted to 2×10^5 cells/mL. Subsequently, the μ -slide was removed from the incubator, and 50 μ L of cell suspension was treated per well (10,000–15,000/well per well). Furthermore, the μ -slide was closed and placed in the incubator for culture. The image was taken using a light microscope DMI8 (Leica) after 8 h.

Flow-cytometric analysis for cell apoptosis detection

Transfected cells (1×10^6) were treated with 0.25% trypsin (1 \times), followed by washing with 2 mL ice-cold PBS. The cell apoptosis was detected using the Annexin V-Fluorescein Isothiocyanate (FITC) Apoptosis Detection Kit (CronDabio, KCD-T2007). Briefly, the cells (1×10^6) were resuspended in 100 μ L of binding buffer and mixed with 5 μ L of Annexin V-FITC and 5 μ L propidium iodide (PI). Then the cells were incubated at 37 $^{\circ}$ C in darkness for 20 min. Cell apoptosis was assessed on a flow cytometer FACS Aria TM III (BD Biosciences, Franklin Lakes, NJ, USA). Cells percentage "Q2 + Q3" was regarded as the apoptotic rate.

Xenograft experiment in nude mice

Lentiviruses expressing either HDAC1-targeting short hairpin RNA (shRNA, sh-HDAC1) or an NC shRNA (sh-NC) were used to obtain a stable HDAC1 knockdown cell line which was selected with 2 μ g/mL puromycin. BALB/c nude mice (6–8 weeks old) were purchased from the Yangzhou University Comparative Medicine Center. Nude mice were kept in the specific pathogen-free (SPF) animal laboratory at 21–23 $^{\circ}$ C and humidity of 60–65% for one week to ready them for cell inoculation in good condition. Moreover, 75% alcohol was used to sterilize the skin of the injection site in nude mice, and 100% of the skin was injected subcutaneously in nude mice with 100 μ L Siha cell suspension (5×10^6 cells). Each group contained three nude mice. The tumor size was examined eve-

ry five days. After 30 days of tumor formation, the nude mice were killed by intravenous injection of an overdose of barbiturates, and then the tumors were separated for photographing and weighing. The volumes of the tumor xenografts were calculated by the formula: Tumor volume (mm^3) = (length \times width 2)/2. For radiotherapy, all mice were irradiated with a single dose of 4 Gy when the tumor diameter reached 4 mm, once a week for four weeks; each mouse received a total dose of 16 Gy. All experimental animal procedures were approved by the Animal Research Ethics Committee of the Affiliated Wuxi People's Hospital of Nanjing Medical University.

Immunohistochemistry (IHC) assay

Clinical CC and adjacent tissues were obtained and embedded and then sliced into 5 μ m sections. The tissue slice was put into xylene and soaked for 20 min for dewaxing. The slice was dehydrated by gradient ethanol and permeabilized by 0.1% Triton x-100. Afterward, the sections were immersed in an antigen repair solution. Furthermore, primary anti-human Ki67 (ab15580, Abcam, 1: 500) or HDAC1 (ab109411, Abcam, 1: 2500) was incubated with the sections for 2 h. The slices were incubated with biotin-labeled secondary antibody IgG (ab6721, 1: 1000, Abcam, USA) for 20 min, followed by treatment with the streptomycin peroxidase solution for 10 min, stained with diaminobenzidine (DAB) for 8 min, and counterstained with hematoxylin for 3 min at room temperature. The images were observed using a light microscope DMI8 (Leica).

TdT-mediated dUTP-biotin nick end-labeling (TUNEL) staining

After tumorigenesis, tumor tissue was harvested from nude mice, fixed with 10% formaldehyde, embedded, and then sliced into a 4 μ m section. The sections were put into xylene for 20 min to dewax. The slice was rehydrated by gradient ethanol. Afterward, the sections were treated with 50 μ L biotin labeling solution for incubation in the dark for 1 hour, followed by treatment with 50 μ L streptavidin HRP working solution for incubation for 30 min. After washing, the sections were colored with 50 μ L of DAB for 10 min. Next, the sections were incubated with hematoxylin staining for 1 min and turned blue after differentiation washing. The staining was observed under a light microscope DMI8 (Leica).

Statistical analysis

Data were analyzed using GraphPad Prism version 7.0 software (GraphPad Software, San Diego, CA, USA). At least three biological repeats were indicated as the mean \pm standard deviation (SD). Student's T-test and ANOVA test were adopted to detect the significance of groups. P-value < 0.05 was statistical significance.

Results

HDAC1 is high-expressed in the CC tumor tissue

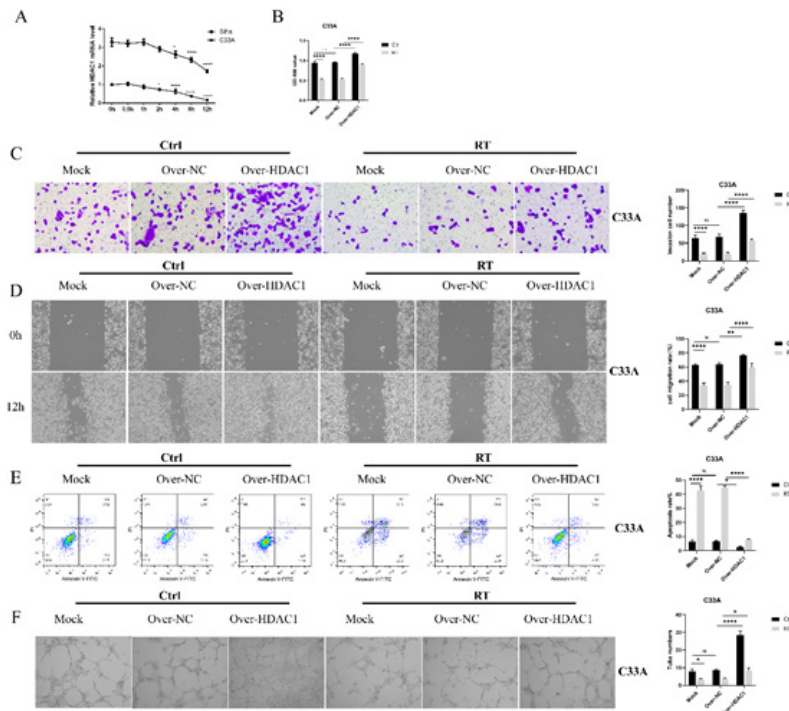
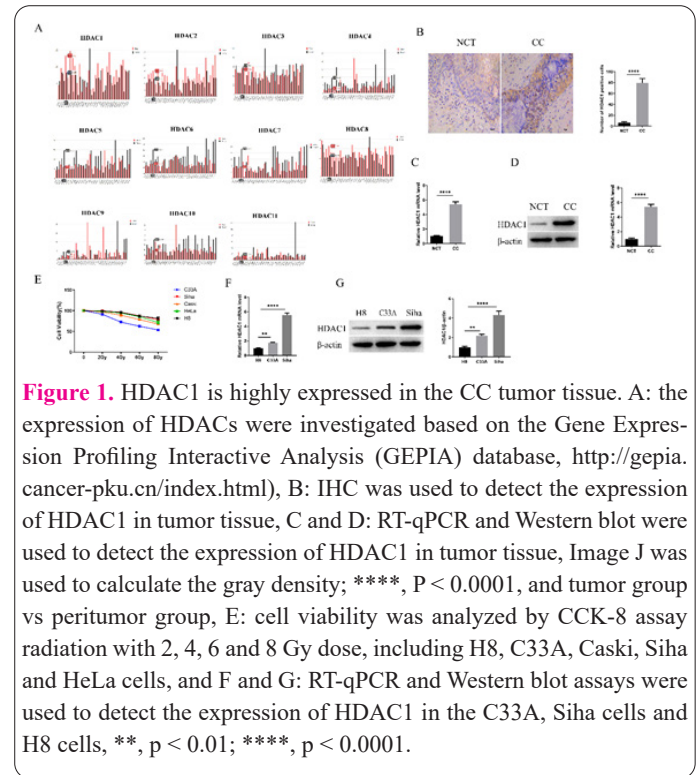
In order to identify the key HDAC1s that may be implicated in CC development, HDACs expression in the CC tumor tissue was investigated on the basis of the GEPIA database (<http://gepia.cancer-pku.cn/index.html>). HDAC1, 2 and 8 expression was separately elevated in the tumor tissues compared to normal tissues. Among them, HDAC1 upregulation was the most obvious (Figure 1A).

Therefore, HDAC1 was selected for further study. Subsequently, the IHC, RT-qPCR and Western blot results suggested that HDAC1 expression was elevated in CC tumor tissue in comparison with NCT (Figures 1B-D). In order to know whether HDAC1 was involved in radiotherapy sensitivity, HDAC1 expression was detected in CC cells with different radiotherapy. As shown in Figure 1E, C33A and Caski cells showed reduced cell viability after 2, 4, 6, and 8 Gy irradiation compared to H8 cervical epithelial cells, while Siha and HeLa cells showed no change in cell viability. C33A and Siha were selected for further study because they were the most sensitive and least sensitive, respectively. RT-qPCR together with Western blot assays displayed that HDAC1 expression was significantly upregulated in the C33A and Siha cells compared with H8 cells. Meanwhile, HDAC1 expression was prominently promoted in Siha cells compared to C33A cells (Figure 1F and G). Collectively, HDAC1 might participate in the radiotherapy sensitivity of CC.

Overexpression of HDAC1 suppresses radiotherapy sensitivity in C33A cells

To confirm whether HDAC1 was related to radiotherapy sensitivity, the half-life of HDAC1 in Siha and C33A cells was detected after radiotherapy. As displayed in Figure 2A, the half-life of HDAC1 was dramatically longer in Siha cells compared to C33A cells. CCK-8 assay suggested that the lessened cell viability in C33A cells caused by radiotherapy was promoted after overexpression of HDAC1 (Figure 2B). Transwell and scratch experiment assays demonstrated that cell invasion and migration were dramatically reduced after radiotherapy, while overex-

pression of HDAC1 promoted the invasion and migration of C33A cells (Figure 2C and D). Flow cytometry assays suggested that radiotherapy-induced increase in C33A cells apoptosis was inhibited upon HDAC1 overexpression (Figure 2E). Tube formation assay demonstrated that the tube-forming potential of C33A cells was dramatically reduced after radiotherapy, while the cell tube-forming



ability of C33A cells was elevated by overexpression of HDAC1 in C33A cells relative to the NC group (Figure 2F). Taken together, HDAC1 elevation suppressed radiotherapy sensitivity in C33A cells.

Knockdown of HDAC1 promotes radiotherapy sensitivity in Siha cell

Subsequently, the function of HDAC1 on radiotherapy sensitivity was detected in Siha cells. As revealed in Figure 3A, in comparison with si-NC, si-HDAC1-2 possessed the highest silencing efficiency, which was selected for subsequent analyses. CCK-8 assay manifested that the inhibited viability of Siha cells stimulated by radiotherapy was further decreased after the knockdown of HDAC1 (Figure 3B). Transwell and scratch experiment assays showed that the invasion and migration capacities of Siha cells were dramatically reduced after radiotherapy. However, silencing of HDAC1 further reduced the invasion and migration of Siha cells (Figures 3C and D). Flow cytometry assays illustrated that the apoptosis in Siha cells was significantly elevated after radiotherapy. Of note, the down-regulation of HDAC1 further promoted apoptosis in Siha cells (Figure 3E). The tube formation experiment displayed that the tube-forming capacity of Siha cells was dramatically lessened after radiotherapy. After HDAC1 knockdown, the tube formation ability of Siha cells was further reduced (Figure 3F). All above data results implied HDAC1 depletion promoted radiotherapy sensitivity in Siha cells.

HDAC1 affects radiotherapy sensitivity by modulating the HIF-1 α -VEGF signaling pathway in CC cells

As reported previously, the HIF-1 α -VEGF signaling pathway has a crucial role in various cancers, including CC (22). However, whether HDAC1 affects radiotherapy sensitivity by modulating HIF-1 α /VEGF signaling pathway remains undefined. Here, levels of HIF-1 α -VEGF signaling pathway-related proteins were assessed. It was revealed that HIF-1 α , VEGFA, together with VEGFR mRNA levels were decreased after radiotherapy both in C33A and Siha cells. Further analysis found that HIF-1 α , VEGFA, along VEGFR expression were dramatically increased with HDAC1 overexpression in C33A cells. Inversely, HIF-1 α , VEGFA, as well as VEGFR expression were lessened in Siha cells with HDAC1 silencing (Figure 4A–F). Similar results were also verified by Western blot (Figure 4G–M). Taken together, HDAC1 influenced radiotherapy sensitivity by regulating HIF-1 α /VEGF signaling pathway.

Knockdown of HDAC1 promotes radiotherapy sensitivity in vivo

In order to further certify the function of HDAC1 in radiotherapy sensitivity for CC, the tumor-bearing nude mice model was established. Tumor volume was significantly decreased at 10 days after tumor-bearing with HDAC1 suppression compared to the NC group with radiotherapy (Figure 5A). Tumor weight in sh-HDAC1 declined compared with the NC group at 30 days after tumorigenesis with radiotherapy (Figure 5B). Ki-67 im-

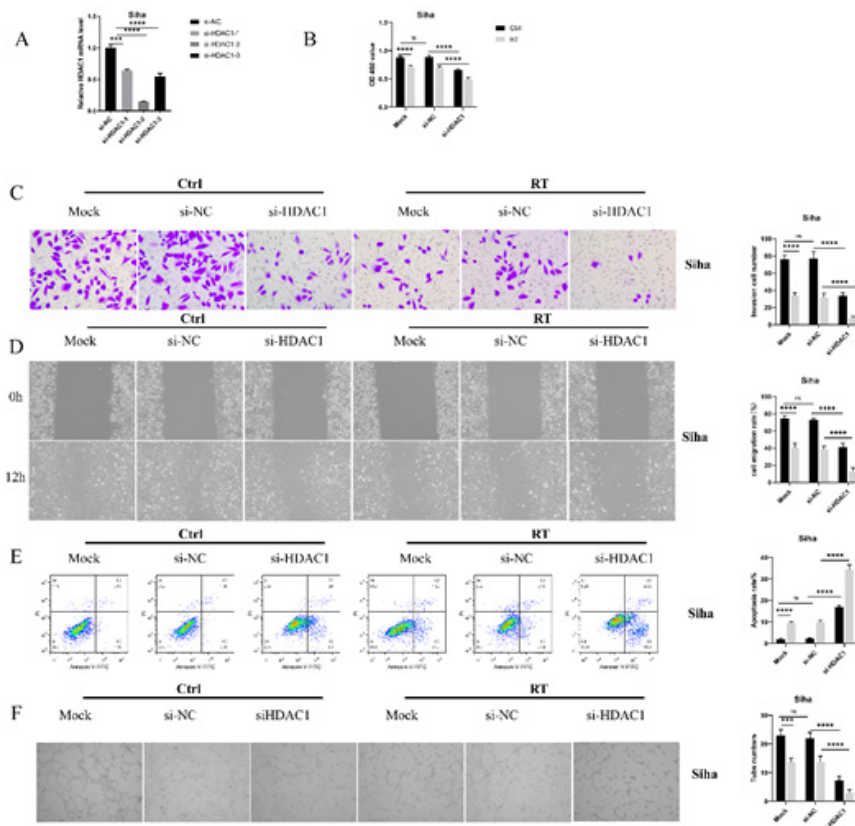
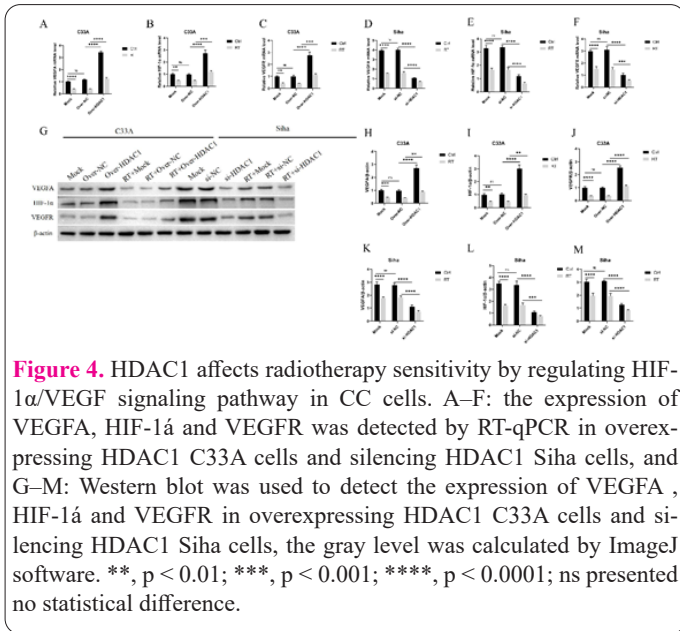


Figure 3. Knockdown of HDAC1 promotes radiotherapy sensitivity in Siha cells. A: RT-qPCR was used to detect the silencing efficiency of siRNA of HDAC1 by transfection with siRNA of HDAC1-1, -2 and -3, respectively, **, $p < 0.01$, si-HDAC1 group vs si-NC group, B: CCK-8 assay was used to detect the cell viability of Siha cells after knockdown of HDAC1, C and D: Transwell and scratch experiment assay was used to detect the cell invasion and migration ability of Siha cells after knockdown of HDAC1, E: flow cytometry assays were used to detect the cell apoptosis after knockdown of HDAC1 in Siha cells, and F: Tube formation assay was used to detect the tube forming ability of Siha cells after knockdown of HDAC1. ***, $p < 0.001$; ****, $p < 0.0001$; ns presented no statistical difference.



munohistochemical staining analysis showed that Ki-67 expression was reduced upon HDAC1 silence, suggesting that silencing of HDAC1 inhibited tumor cell proliferation (Figure 5C). TUNEL assay showed that the apoptosis was prominently increased with HDAC1 silence (Figure 5D). These outcomes revealed that HDAC1 reduction promoted radiotherapy sensitivity in vivo.

HDAC1 affects radiotherapy sensitivity by modulating HIF-1 α /VEGF signaling pathway in vivo

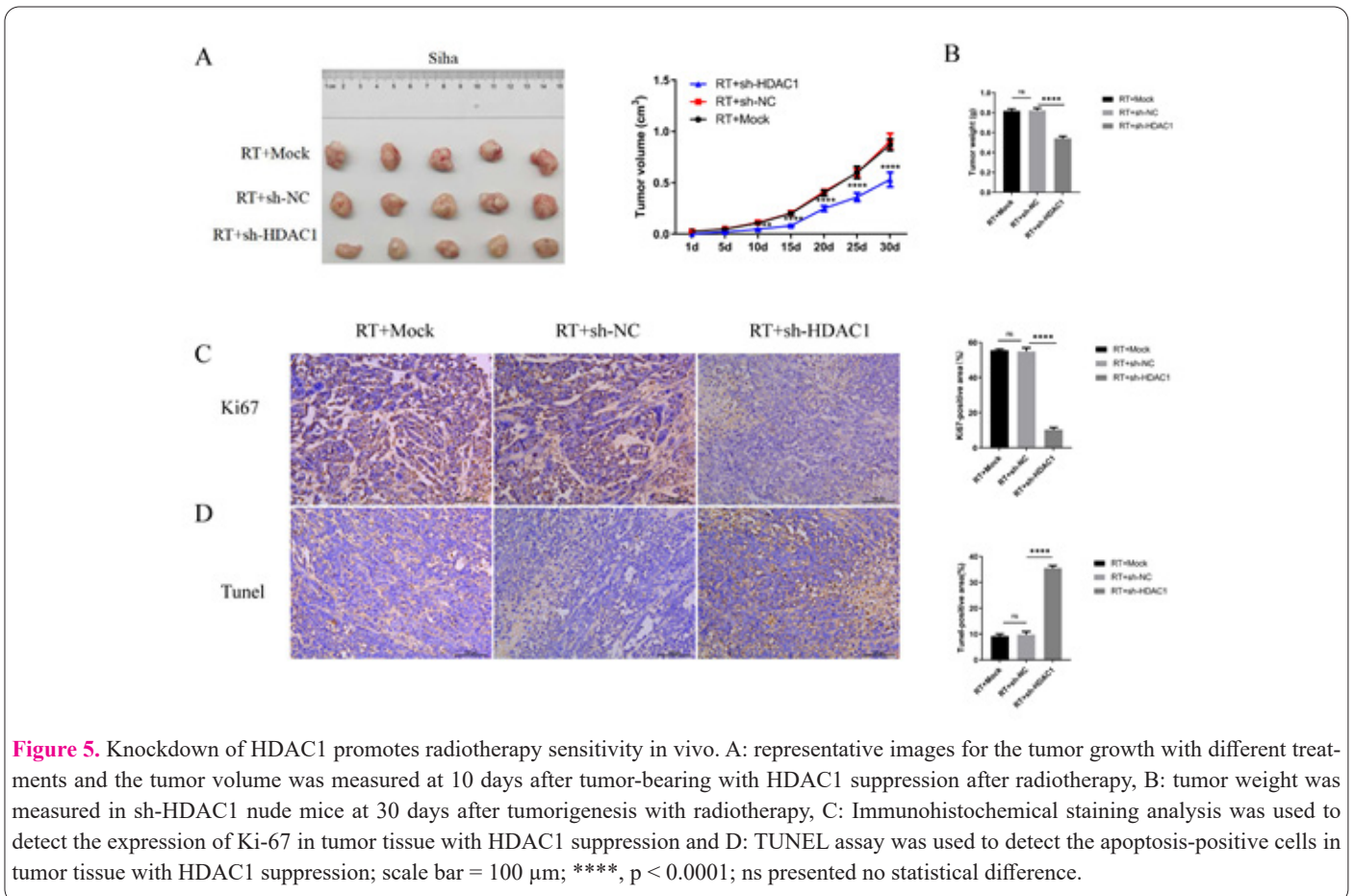
Moreover, we investigated whether HIF-1 α /VEGF signaling pathway was affected by HDAC1 in vivo. As shown in Figure 6A–C, RT-qPCR assay found that HIF-

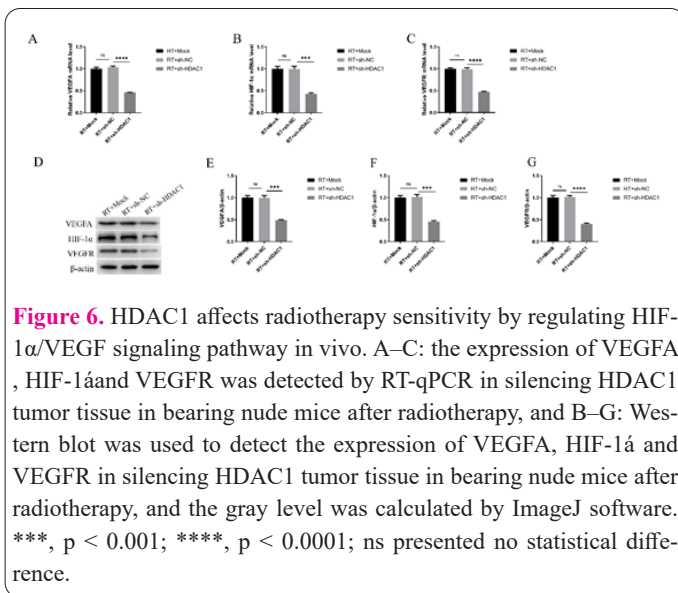
1 α , VEGFA, and VEGFR expression was significantly decreased at mRNA level in HDAC1-silenced tumor tissues of nude mice after radiotherapy. Western blot also showed that HIF-1 α , VEGFA, and VEGFR were decreased at the protein level in HDAC1-silenced tumor tissues compared with the NC group in nude mice after radiotherapy (Figure 6D–G). These results indicated that HDAC1 affected radiotherapy sensitivity through modulating the HIF-1 α /VEGF signaling pathway in vivo.

Discussion

CC has become the fourth most common female malignant tumor affecting women’s health (4). Radiotherapy is the mainstay treatment for CC. However, some patients had poor clinical outcomes due to a lack of radiosensitivity for CC (23). Therefore, it is significant to seek and clarify the mechanism of the key factors of radiotherapy for CC. In the present work, HDAC1 was high-expressed in the tumor tissue and CC cells. Furthermore, we demonstrated that the knockdown of HDAC1 promoted radiotherapy sensitivity in vivo and in vivo via modulating the HIF-1 α /VEGF signaling pathway. These findings provide a therapeutic strategy for boosting CC radiosensitivity.

HDACs harbor a crucial role in chromatin remodeling, gene repression, cell cycle regulation as well and differentiation (24). The abnormal function of HDAC in tumor cells can inhibit gene transcription as well as the expression of tumor suppressor genes (25). The high expression of HDAC1 in tumor cells can increase tumor cell proliferation, and the high expression of HDAC1 can affect the extracellular matrix, which can significantly enhance tumor cell motility (26-28). These data mirrors that HDAC1 plays a crucial role in tumor development. Several reports





have also proved that HDAC1 participates in the regulation of CC progression. Saad et al. have demonstrated that fucoidan can be a therapeutic molecule for CC by targeting HDACs (29). Recently, HDAC1 is screened as a hub gene in the Gene Expression Omnibus (GEO) and TCGA databases as the potential predictor for CC. These outcomes recommend the importance of HDAC1 in CC (30). Consistent with these findings, HDAC1 was high-expressed in the tumor tissue together with C33A and Siha cells of CC. Nevertheless, few studies have focused on the radiotherapy of CC by targeting HDAC1. In the present research, we established that overexpressed HDAC1 suppressed radiotherapy sensitivity in C33A cells while knockdown of HDAC1 promoted radiotherapy sensitivity in Siha cells and in vivo. These results confirmed that HDAC1 silencing promoted radiotherapy sensitivity, providing a new strategy for the radiotherapy of CC. Consistently, it has been documented that HDAC1 is a potent factor resulting in decreased sensitivity of laryngeal squamous cell carcinoma in radiotherapy (31).

The occurrence of malignant tumors is linked to the excessive proliferation of cells, and tumor proliferation requires a lot of oxygen consumption; hypoxia of tumor tissue is an important biological feature of malignant tumors. Many genes in tumor cells responding to hypoxia are regulated by HIF-1 α . Literatures have shown that HIF-1 α is closely related to tumor growth, proliferation, invasion, metastasis, angiogenesis, apoptosis, drug resistance, and other characteristics. VEGF plays a key part in tumor angiogenesis and multiple roles in different cancers after radiotherapy, such as prognostic markers, imaging targets and targeted therapy combined with radiotherapy (32-35). HIF-1 α has a central role in regulating the signal transduction pathway of VEGF during hypoxia, increasing the stability of VEGF mRNA and the transcription activity of VEGF. It has been reported that the HIF-1 α /VEGF signaling pathway is implicated in the progression of CC (36). Jae-Moon Shin et al have pointed that melittin inhibits CC progression and angiogenesis by inhibiting the HIF-1 α /VEGF signaling pathway (37). Some studies have reported the involvement of HIF-1 α in radiotherapy response. Furthermore, Koukourakis et al. have verified that HIF-1 α together with -2 α responds to photodynamic therapy and radiotherapy in early esophageal cancer (38). Wach-

ters et al. have proved that HIF-1 α , CA-IX, along with OPN show prognostic significance in T1-T2 laryngeal carcinoma treated with radiotherapy (39). Recently, Guo et al. have confirmed that baicalein promotes radiosensitivity of esophageal squamous cell carcinoma (ESCC) through regulating HIF-1 α , inhibiting ESCC progression (40). These results suggest that HIF-1 α /VEGF signaling pathway has an important role in response to radiotherapy. However, there are few studies fixated on radiotherapy for CC by targeting HIF-1 α /VEGF signaling pathway. Of note, previous literatures have indicated that HDAC1 activates HIF1 α /VEGFA signal pathway in colorectal cancer (41). In the current research, HIF-1 α , VEGFA, and VEGFR expression were significantly decreased with HDAC1 knockdown after radiotherapy in vitro and in vivo. All the above data implied that HDAC1 affected radiotherapy sensitivity via modulating the HIF-1 α /VEGF signaling pathway.

However, there are some limitations in this study. First, the prognostic value of HDAC1 in CC patients with radiotherapy is unclear. Besides, the cooperation between HDAC1, HIF-1 α , and VEGF-A on the molecular mechanism needs to be further elucidated.

Conclusion

In conclusion, we demonstrated that the elevation of HDAC1 contributed to reducing the radiotherapy sensitivity of CC by modulating the HIF-1 α /VEGF signaling pathway. These findings may provide new insights to develop effective interventions targeting HDAC1 for CC patients undergoing radiotherapy.

Interest conflict

The authors report no conflict of interest.

Consent for publications

The author read and proved the final manuscript for publication.

Availability of data and material

All data generated during this study are included in this published article.

Ethics approval and consent to participate

No human or animals were used in the present research.

Acknowledgements

This study was supported by grants from the Wuxi Taihu Lake Talent Plan, Supports for Leading Talents in Medical and Health Profession, Project plan of Wuxi Institute of translational medicine (LCYJ202210), Scientific Research Project of Wuxi Commission of Health (M202041), Maternal and Child Health Research Project of Jiangsu Commission of Health (F202009).

References

1. Buskwofie A, David-West G, Clare CA. A Review of Cervical Cancer: Incidence and Disparities. *J Natl Med Assoc.* 2020;112:229-32.
2. Johnson CA, James D, Marzan A, Armaos M. Cervical Cancer: An Overview of Pathophysiology and Management. *Semin Oncol Nurs.* 2019;35:166-74.
3. Olusola P, Banerjee HN, Phillely JV, Dasgupta S. Human Papil-

- loma Virus-Associated Cervical Cancer and Health Disparities. Cells. 2019;8.
4. Volkova LV, Pashov AI, Omelchuk NN. Cervical Carcinoma: Oncobiology and Biomarkers. *Int J Mol Sci.* 2021;22.
 5. Tsikouras P, Zervoudis S, Manav B, Tomara E, Iatrakis G, Romanidis C, et al. Cervical cancer: screening, diagnosis and staging. *J BUON.* 2016;21:320-5.
 6. Sharma S, Deep A, Sharma AK. Current Treatment for Cervical Cancer: An Update. *Anticancer Agents Med Chem.* 2020;20:1768-79.
 7. Chargari C, Peignaux K, Escande A, Renard S, Lafond C, Petit A, et al. Radiotherapy of cervical cancer. *Cancer Radiother.* 2022;26:298-308.
 8. Willis-Martinez D, Richards HW, Timchenko NA, Medrano EE. Role of HDAC1 in senescence, aging, and cancer. *Exp Gerontol.* 2010;45:279-85.
 9. Haberland M, Montgomery RL, Olson EN. The many roles of histone deacetylases in development and physiology: implications for disease and therapy. *Nat Rev Genet.* 2009;10:32-42.
 10. Song C, Zhu S, Wu C, Kang J. Histone deacetylase (HDAC) 10 suppresses cervical cancer metastasis through inhibition of matrix metalloproteinase (MMP) 2 and 9 expression. *J Biol Chem.* 2013;288:28021-33.
 11. Wagner W, Ciszewski WM, Kania KD. L- and D-lactate enhance DNA repair and modulate the resistance of cervical carcinoma cells to anticancer drugs via histone deacetylase inhibition and hydroxycarboxylic acid receptor 1 activation. *Cell Commun Signal.* 2015;13:36.
 12. Anantharaju PG, Reddy DB, Padukudru MA, Chitturi CMK, Vimalambike MG, Madhunapantula SV. Induction of colon and cervical cancer cell death by cinnamic acid derivatives is mediated through the inhibition of Histone Deacetylases (HDAC). *PLoS One.* 2017;12:e0186208.
 13. Datta A, West C, O'Connor JPB, Choudhury A, Hoskin P. Impact of hypoxia on cervical cancer outcomes. *Int J Gynecol Cancer.* 2021;31:1459-70.
 14. Serebrovska ZO, Chong EY, Serebrovska TV, Tumanovska LV, Xi L. Hypoxia, HIF-1 α , and COVID-19: from pathogenic factors to potential therapeutic targets. *Acta Pharmacol Sin.* 2020;41:1539-46.
 15. Zhang D, Lv FL, Wang GH. Effects of HIF-1 α on diabetic retinopathy angiogenesis and VEGF expression. *Eur Rev Med Pharmacol Sci.* 2018;22:5071-6.
 16. Chakraborty C, Mitra S, Roychowdhury A, Samadder S, Dutta S, Roy A, et al. Deregulation of LIMD1-VHL-HIF-1 α -VEGF pathway is associated with different stages of cervical cancer. *Biochem J.* 2018;475:1793-806.
 17. Choi SR, Hwang CY, Lee J, Cho KH. Network Analysis Identifies Regulators of Basal-Like Breast Cancer Reprogramming and Endocrine Therapy Vulnerability. *Cancer Res.* 2022;82:320-33.
 18. Lee HY, Tang DW, Liu CY, Cho EC. A novel HDAC1/2 inhibitor suppresses colorectal cancer through apoptosis induction and cell cycle regulation. *Chem Biol Interact.* 2022;352:109778.
 19. Rivas M, Johnston ME, 2nd, Gulati R, Kumbaji M, Margues Aguiar TF, Timchenko L, et al. HDAC1-Dependent Repression of Markers of Hepatocytes and P21 Is Involved in Development of Pediatric Liver Cancer. *Cell Mol Gastroenterol Hepatol.* 2021;12:1669-82.
 20. Ali Khan M, Kedhari Sundaram M, Hamza A, Quraishi U, Gunasekera D, Ramesh L, et al. Sulforaphane Reverses the Expression of Various Tumor Suppressor Genes by Targeting DNMT3B and HDAC1 in Human Cervical Cancer Cells. *Evid Based Complement Alternat Med.* 2015;2015:412149.
 21. Sixto-Lopez Y, Rosales-Hernandez MC, Contis-Montes de Oca A, Fragoso-Morales LG, Mendieta-Wejebe JE, Correa-Basurto AM, et al. N-(2'-Hydroxyphenyl)-2-Propylpentanamide (HO-AAVPA) Inhibits HDAC1 and Increases the Translocation of HMGB1 Levels in Human Cervical Cancer Cells. *Int J Mol Sci.* 2020;21.
 22. Zhang W, Xiong Z, Wei T, Li Q, Tan Y, Ling L, et al. Nuclear factor 90 promotes angiogenesis by regulating HIF-1 α /VEGF-A expression through the PI3K/Akt signaling pathway in human cervical cancer. *Cell Death Dis.* 2018;9:276.
 23. Naga Ch P, Gurram L, Chopra S, Mahantshetty U. The management of locally advanced cervical cancer. *Curr Opin Oncol.* 2018;30:323-9.
 24. King J, Patel M, Chandrasekaran S. Metabolism, HDACs, and HDAC Inhibitors: A Systems Biology Perspective. *Metabolites.* 2021;11.
 25. Dunaway LS, Pollock JS. HDAC1: an environmental sensor regulating endothelial function. *Cardiovasc Res.* 2022;118:1885-903.
 26. Brancolini C, Gagliano T, Minisini M. HDACs and the epigenetic plasticity of cancer cells: Target the complexity. *Pharmacol Ther.* 2022;238:108190.
 27. Singh T, Kaur P, Singh P, Singh S, Munshi A. Differential molecular mechanistic behavior of HDACs in cancer progression. *Med Oncol.* 2022;39:171.
 28. Hai R, Yang D, Zheng F, Wang W, Han X, Bode AM, et al. The emerging roles of HDACs and their therapeutic implications in cancer. *Eur J Pharmacol.* 2022;931:175216.
 29. Mustafa S, Pawar JS, Ghosh I. Fucoidan induces ROS-dependent epigenetic modulation in cervical cancer HeLa cell. *Int J Biol Macromol.* 2021;181:180-92.
 30. Tu S, Zhang H, Yang X, Wen W, Song K, Yu X, et al. Screening of cervical cancer-related hub genes based on comprehensive bioinformatics analysis. *Cancer Biomark.* 2021;32:303-15.
 31. Zhao R, Chen K, Cao J, Yu H, Tian L, Liu M. A correlation analysis between HDAC1 over-expression and clinical features of laryngeal squamous cell carcinoma. *Acta Otolaryngol.* 2016;136:172-6.
 32. Harmankaya I, Caloglu VY, Tastekin E, Turkkan G, Caloglu M, Uzal C. Prognostic importance of microvessel density, VEGF expression and perineural invasion in laryngeal cancer treated with adjuvant radiotherapy. *Indian J Pathol Microbiol.* 2022;65:521-6.
 33. Zlobec I, Vuong T, Compton CC, Lugli A, Michel RP, Hayashi S, et al. Combined analysis of VEGF and EGFR predicts complete tumour response in rectal cancer treated with preoperative radiotherapy. *Br J Cancer.* 2008;98:450-6.
 34. Kanthou C, Tozer G. Targeting the vasculature of tumours: combining VEGF pathway inhibitors with radiotherapy. *Br J Radiol.* 2019;92:20180405.
 35. Rybalov, Maxim, Ananias, Hildo JK, Hoving, Hilde D, et al. PSMA, EpCAM, VEGF and GRPR as Imaging Targets in Locally Recurrent Prostate Cancer after Radiotherapy.
 36. Zhao Y, You W, Zheng J, Chi Y, Tang W, Du R. Valproic acid inhibits the angiogenic potential of cervical cancer cells via HIF-1 α /VEGF signals. *Clin Transl Oncol.* 2016;18:1123-30.
 37. Shin JM, Jeong YJ, Cho HJ, Park KK, Chung IK, Lee IK, et al. Melittin suppresses HIF-1 α /VEGF expression through inhibition of ERK and mTOR/p70S6K pathway in human cervical carcinoma cells. *PLoS One.* 2013;8:e69380.
 38. Koukourakis MI, Giatromanolaki A, Skarlatos J, Corti L, Blandamura S, Piazza M, et al. Hypoxia inducible factor (HIF-1 α and HIF-2 α) expression in early esophageal cancer and response to photodynamic therapy and radiotherapy. *Cancer Res.* 2001;61:1830-2.
 39. Wachters JE, Schrijvers ML, Slagter-Menkema L, Mastik M, de Bock GH, Langendijk JA, et al. Prognostic significance of HIF-1 α , CA-IX, and OPN in T1-T2 laryngeal carcinoma treated with

- radiotherapy. *Laryngoscope*. 2013;123:2154-60.
40. Guo D, Jin J, Liu J, Wang Y, Li D, He Y. Baicalein Inhibits the Progression and Promotes Radiosensitivity of Esophageal Squamous Cell Carcinoma by Targeting HIF-1A. *Drug Des Devel Ther*. 2022;16:2423-36.
41. Chen C, Wei M, Wang C, Sun D, Liu P, Zhong X, et al. The histone deacetylase HDAC1 activates HIF1 α /VEGFA signal pathway in colorectal cancer. *Gene*. 2020;754:144851.